

Modelling skull dynamics during brain magnetic resonance elastography to evaluate wave delivery strategies

Deirdre M McGrath^{1,2}, Alejandro F Frangi¹, Iain D Wilkinson², and Zeike A Taylor¹

¹CISTIB, Center for Computational Imaging & Simulation Technologies in Biomedicine, University of Sheffield, Sheffield, South Yorkshire, United Kingdom, ²Academic Radiology, University of Sheffield, Sheffield, South Yorkshire, United Kingdom

TARGET AUDIENCE: Magnetic resonance elastography researchers developing methodology for brain.

PURPOSE: Magnetic resonance elastography (MRE) is currently being explored as a biomarker of neurodegenerative disease including dementia^{1,2}. A difficulty for this process of evaluation is that the measures of biomechanical properties obtained for healthy brain using MRE have varied widely³. However the methodology has not been consistent between studies, such as wave frequency and the means of wave delivery, e.g., bite-bar⁴, via the temples, back of the head¹, head cradle⁵ etc. It is therefore important to examine the possible impact of varying the delivery route. In this work an initial evaluation of has been made of a method to simulate skull vibration dynamics during MRE. 3D finite element model (FEM) based simulations have been carried out to simulate vibrations through the cranium from various delivery positions.

METHODS: MRE was simulated in a human skull model using Abaqus v6.12 (Dassault Systèmes Simulia Corp, Providence, RI) with the harmonic direct-solution steady-state dynamic analysis function at frequencies previously employed for brain MRE (Table 1, 4,5). In this algorithm harmonic response is calculated in terms of the physical degrees of freedom of the model using the mass, damping, and stiffness matrices of the system and solving the dynamic virtual work equation: $\int_V \rho \delta u \cdot \ddot{u} dV + \int_V \rho \alpha \delta u \cdot \dot{u} dV + \int_V \delta \epsilon : \sigma dV - \int_{S_t} \delta u \cdot t dS = 0$, where \dot{u} and \ddot{u} are the velocity and acceleration, ρ is the material density, α is the mass proportional damping factor, σ is the stress, t the surface traction, $\delta \epsilon$ the strain variation corresponding to the displacement variation δu , V the volume and S_t the surface. The output of the algorithm is the frequency domain complex displacement field u , $\Delta u = (\Re(u) + i\Im(u)) \exp i\omega t$, where ω is the circular frequency. The model was meshed from the XCAT Phantom⁶ using linear tetrahedral elements (77,000 nodes, 328,000 elements). The skull was modelled as an elastic solid with properties set to those of previous FEM simulations for cortical bone⁷ (Table 2), and a density of 1500 kg/m³. The applied boundary conditions of the simulation included harmonic displacement of 100µm amplitude in various directions

Table 1: Frequencies (Hz)
25
37.5
50
62.5
90

Table 2: Cranium mechanical properties	
E (MPa)	Poisson's ratio
15.000	0.21

applied to the nodes corresponding to the various points of wave delivery (Fig. 1, Table 3). The skull was tethered using zero displacement boundary conditions at the cranial nodes surrounding the neck.

RESULTS: The displacement magnitudes at the nodes for the varying wave delivery schemes at 25 and 90 Hz (the extremes of the 5 frequencies employed) are visualised in Fig.2. The results demonstrate how the displacement amplitudes and wave patterns in the skull can vary greatly depending on the mode of wave delivery. Fig. 3 plots the maximum

displacement magnitude of the nodes on the inside surface of the cranium (nodes nearest the brain), against frequency, and for the various wave delivery options. The maximum displacement increases slightly with frequency for each option. Option A (head cradle, head-foot displacement) resulted in the maximum displacement, while option E (bite-bar) resulted in the lowest. Although options C and D were very different methods (head cradle, left-right displacement of the

temples in the same direction, and acoustic pillow) they resulted in a similar maximum displacement magnitude at all frequencies. Option B (head cradle, left-right, opposite directions) resulted in medium values but showed the most dependency on frequency.

DISCUSSION: These initial results provide new insight into the patterns of displacements in the skull generated during MRE. They demonstrate that the different delivery routes and frequencies of vibration can result in very different outcomes in terms of the vibration reaching the inner surface of the cranium next to the brain. However the data also shows that some very different delivery options can result in very similar outcomes. The optimum method from these simulations would appear to be the head cradle moving the temples in the head-foot direction. However more work is needed to establish the limits of these findings. For instance only one skull model from one individual was used. Also, although bone consists of both cortical and cancellous bone types, only cortical bone has been modelled here, and moreover no material damping term was provided. Also no account was made of the damping effect of the surrounding soft tissue such as skin, fat and muscle. Furthermore any dependency on mesh density and element type needs to be established. Indeed, the mechanism of wave delivery to the brain via the skull in MRE is not well understood, but is likely to occur via a combination of mechanical vibration of the structures of the meninges and the processes of the dura mater (*falx cerebri* and *tentorium cerebelli*) and acoustic waves through the cerebral spinal fluid. After exploring the proposed variations in the simulations outlined above, the next step would be to translate the skull displacements to the brain for MRE simulation. Through comparison with acquired MRE data, the task will be to determine which mechanisms govern the delivery of wave energy to the brain. This will inform the development of optimum wave delivery strategies for MRE, and furthermore will provide important insight into how the structures within the cranium respond to mechanical waves.

CONCLUSION: The displacement amplitudes and wave patterns through the skull induced during MRE can vary greatly depending on the site of wave delivery. However within the typical range of frequencies employed for MRE these patterns appear less dependent on frequency. The data obtained from this study will inform further simulations to determine the optimum wave delivery strategies for MRE.

References:[1] Murphy, et al., J Magn Reson Im 2011. 34: p. 494-498; [2] Lipp, et al., Neuroimage Clin, 2013; 3: p. 381-7; [3] Di Ieva, A., et al., Neurosurg Rev, 2010. 33(2): p. 137-45; [4] Green, et a. NMR Biomed, 2008. 21(7): p. 755-64; [5] Sack, et al., Neuroimage, 2009. 46(3): p. 652-7.; [6] Segars et al., 2010, Med Phys, 37(9),4902-4915; [7] Wittek, et al. 2011, Computational Biomechanics for Medicine, Soft Tissues and the Muskuloskeletal System, Springer

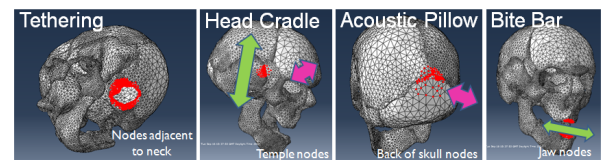


Figure 1: Boundary conditions for wave delivery options

Table 3: Wave delivery methods		
Name	Device	Description
A	Head cradle	Temples pushed in head-foot direction
B	Head cradle	Temples pushed left-right in opposite directions
C	Head cradle	Temples pushed left-right in same direction
D	Acoustic pillow	Nodes at back of skull pushed in anterior-posterior direction
E	Bite bar	Nodes on upper and lower jaw pushed left-right

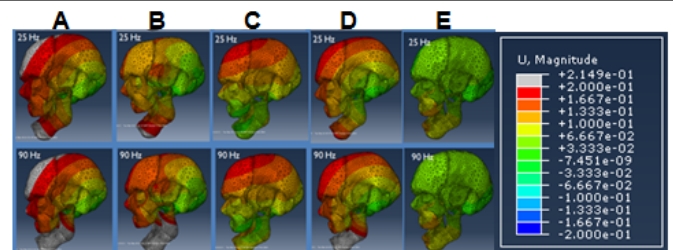


Figure 2: Displacement magnitudes for wave delivery options

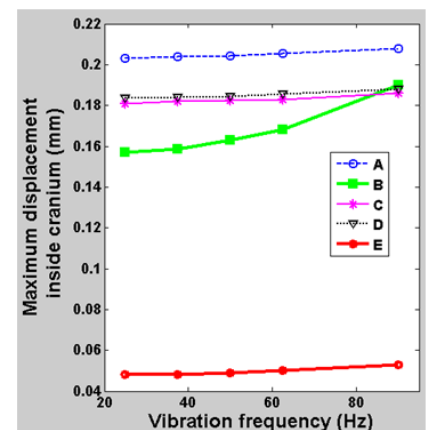


Figure 3: Maximum displacement magnitude on the inside of the cranium against vibration frequency for the different wave delivery options.